Decentralized H2 observers for position and velocity estimation in vehicle formations with fixed topologies

Daniel Viegas, Pedro Batista, Paulo Oliveira, and Carlos Silvestre

Systems & Control Letters, vol. 61, no. 3, pp. 443-453, March 2012

https://doi.org/10.1016/j.sysconle.2011.12.004

Decentralized H_2 observers for position and velocity estimation in vehicle formations with fixed topologies

Daniel Viegas*, Pedro Batista, Paulo Oliveira, Carlos Silvestre

Institute for Systems and Robotics, Instituto Superior Técnico, Universidade Técnica de Lisboa
Av. Rovisco Pais, 1049-001 Lisboa, Portugal

Abstract

This paper addresses the problem of decentralized state estimation in fixed topology formations of vehicles with applications to Autonomous Underwater Vehicles (AUVs). In the envisioned scenario, each vehicle in the formation estimates its own state relying only on locally available measurements and data communicated by neighboring agents, requiring lower computational and communication loads than centralized solutions. A method for designing local state observers featuring global error dynamics that converge globally asymptotically to zero is detailed, and an algorithm for improving its performance under stochastic disturbances and Gaussian uncertainties is presented. The proposed algorithm minimizes the H_2 norm of the global estimation error dynamics, expressed as an optimization problem subject to Bilinear Matrix Inequality (BMI) constraints. To assess the performance of the solution, realistic simulation results are presented and discussed for several formation topologies.

Keywords: Cooperative navigation, Decentralized estimation, Autonomous vehicles

1. Introduction

The increasing use of formations in robotics, as well as the evolution of parallel computing, have led to extensive research in the field of distributed systems and agent formations, see e.g. [1, 2, 3, 4]. In short, a distributed system consists of multiple autonomous computers or agents that communicate information between them and work towards a common goal. The wealth of possible scenarios, as well as the increased complexity that results from the interactions between multiple agents, has led to many compelling approaches and contributions in the past few years, both in the field of control [5, 6] and of estimation [7, 8] in multi-agent formations.

There are many applications where the use of multiple agents in a cooperative setting is beneficial or even crucial. Unmanned Aerial Vehicles (UAVs) can be used in a formation setting advantageously, as close formation flight reduces drag, thus allowing for more efficient fuel usage [9, 10]. In underwater applications, the concerted operation of formations of Autonomous Underwater Vehicles (AUVs) has many potential applications, such as minesweeping and oceanographic sampling [11, 12]. Automated highway systems also pose several problems related to formations, such as collision avoidance and traffic flow control [13, 14]. In general, any task where a single agent is too slow or does not offer enough coverage, and any setting where multiple autonomous agents are present, may benefit from the study of the problem under a distributed point of view. One might wonder why the problems related with formations should be treated in a distributed setting when their treatment in a global, centralized way might probably be much simpler conceptually. However, the computations involved with large formations are often very heavy and would require much higher processing power of the agents, which is a problem when dealing with size and energy concerns, and would need the extensive use of telecommunications to and from a central processing node. Alternatively, a central computer could perform all the computations and spread them through the formation by communication, but it could cause unacceptable delays and communication loads.

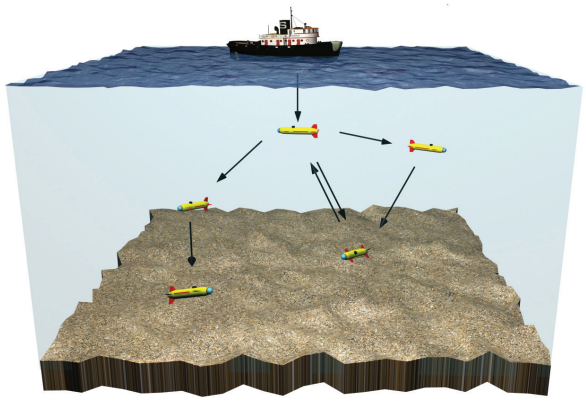

Figure 1: Formation of AUVs working underwater

This paper addresses the problem of state estimation of linear motion quantities in a formation of vehicles in a distributed

*Corresponding author
Email addresses: dviegas@isr.ist.utl.pt (Daniel Viegas), pbatista@isr.ist.utl.pt (Pedro Batista), pjcro@isr.ist.utl.pt (Paulo Oliveira), cjs@isr.ist.utl.pt (Carlos Silvestre)

setting. Each agent in the formation aims to estimate its own position based on some awareness of its own movement and local measurements and communications. In the specific case treated in this paper, each agent has access to either measurements of its absolute position, or measurements of its position relative to one or more agents, as well as the state estimates of those agents, received through communication. Additionally, awareness of its own movement is given by a measure of its linear acceleration, provided by an accelerometer mounted on-board, and an Attitude and Heading Reference System (AHRS), which gives the attitude and angular velocity of the vehicle. This problem is especially relevant in the scenario of a formation of AUVs working underwater such as the one depicted in Fig. 1, as sophisticated navigation solutions such as the Global Positioning System (GPS) are impractical due to the attenuation of electromagnetic waves in water. For a recent, detailed survey on the subject of underwater navigation, see [15]. In this setting, one or more agents could have access to measurements of their absolute position using, e.g., range readings to a fixed source or to a series of beacons [16, 17]. The other agents would then rely on locally available measurements and data communication to estimate their own position. A method for local state observer design, rooted in classical state observer theory, is presented here, and the estimation error of the distributed state observer composed by the local estimators that are implemented in each agent of the formation is shown to converge globally asymptotically to zero for a certain class of formation structures. Namely, in the structures first considered there is no communication feedback between the agents, that is, the information flows in a single direction, and this allows for the design of the local observers based only on local dynamics. Building on this, an iterative algorithm, inspired by the $\mathcal{P}-\mathcal{K}$ iterations used in some controller synthesis problems [18, 19], is presented for improving the performance of such a decentralized observer in noisy environments, as well as constructively incorporating additional measurements and communication that may create information loops in the formation, based on the minimization of the H_2 norm of the estimation error dynamics. This problem is formulated as an optimization problem with bilinear matrix inequality (BMI) constraints. To the best of the authors' knowledge, this is the first work on decentralized navigation with globally asymptotic stability and performance guarantees for arbitrary fixed formation topologies, especially with cycles in the formation graph.

The paper is organized as follows: Section 2 details the problem at hand and introduces the dynamics of the agents and of the local state observers, while Section 3 analyzes the convergence properties of the distributed state observer formed by the simultaneous implementation of local state observers by each agent in a formation. Section 4 formulates the problem of optimal decentralized state estimation as an optimization problem with BMI constraints, and presents an iterative algorithm to improve the performance of the decentralized state observer. Section 5 details an extension of the results presented in the previous sections to alternative scenarios and Section 6 shows the results of several simulations carried out to assess the performance of the proposed solution. Finally, Section 7 summarizes the main conclusions of the paper.

1.1. Notation

Throughout the paper the symbol $\mathbf{0}$ denotes a matrix (or vector) of zeros and $\mathbf{I}$ an identity matrix, both of appropriate dimensions. Whenever relevant, the dimensions of an $n \times n$ identity matrix are indicated as $\mathbf{I}_n$. A block diagonal matrix is represented as $\mathrm{diag}\,(\mathbf{A}_1, \ldots, \mathbf{A}_\mathrm{n})$, and the Kronecker product of two matrices $\mathbf{A}$ and $\mathbf{B}$ is denoted by $\mathbf{A} \otimes \mathbf{B}$. For $\mathbf{x}, \mathbf{y} \in \mathbb{R}^3$, $\mathbf{x} \times \mathbf{y}$ represents the cross product.

2. Problem Statement

Consider a formation composed by N agents moving in a scenario, where each agent is identified by a distinct positive integer $i \in \{1, 2, \ldots, N\}$, and has sensors mounted on-board which give access to either:

1. measurements of its own position in an inertial reference coordinate frame $\{I\}$; or
2. measurements of its position relative to one or more agents in the vicinity, denoted in the sequel as the source-agents of agent i. Furthermore, each of those agents transmits an estimate of its own inertial position to agent i.

It is assumed that the topology of the formation is fixed, in the sense that the measurements and communication available to each agent do not change over the course of the mission. Besides the transmission of position estimates that goes with the relative position measurements, no further communication is assumed. The relative measurements can be provided by vision-based or range-based sensors for aerial or ground vehicles, and by an Ultra-short Baseline (USBL) positioning system in an inverted configuration in underwater applications. The USBL is composed of a small calibrated array of acoustic receivers and measures the distance between a transponder and the receivers, from which the relative position can be recovered [20]. The inertial measurements can be provided, e.g., by a GPS, a Long Baseline (LBL), or by an USBL positioning system.

The problem considered in this paper is the design of a decentralized solution that allows each agent in the formation to estimate its own inertial position and velocity. The approach described here, schematized in Fig. 2 for a simple formation, consists in the implementation of a local state estimator on-board each agent. While the design and calibration of those local state estimators will be carried out before the mission in an external processing node, during operation each agent will only require locally available measurements to estimate its state, along with the aforementioned limited communication.

2.1. Agent Dynamics

Let $\{B_i\}$ denote a coordinate frame attached to agent i, denominated in the sequel as the body-fixed coordinate frame associated with the i-th agent. The linear motion of agent i can be written as

$$\dot{\mathbf{p}}_i(t) = \mathbf{R}_i(t)\mathbf{v}_i(t), \tag{1}$$

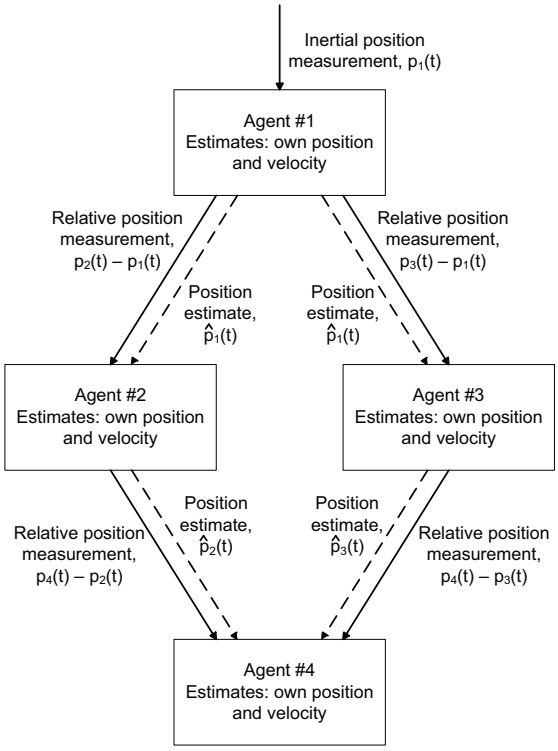

Figure 2: Schematic representation of a simple formation of 4 agents. Dotted arrows represent communication of state estimates, while full arrows represent absolute and relative position measurements.

where $\mathbf{p}_i(t) \in \mathbb{R}^3$ is the inertial position of the agent, $\mathbf{v}_i(t) \in \mathbb{R}^3$ denotes its velocity relative to $\{I\}$, expressed in body-fixed coordinates of the i-th agent, and $\mathbf{R}_i(t) \in SO(3)$ is the rotation matrix from $\{B_i\}$ to $\{I\}$, which satisfies

$$\dot{\mathbf{R}}_i(t) = \mathbf{R}_i(t)\mathbf{S}(\boldsymbol{\omega}_i(t)),$$

where $\boldsymbol{\omega}_i(t) \in \mathbb{R}^3$ is the angular velocity of $\{B_i\}$, expressed in body-fixed coordinates of the i-th agent, and $\mathbf{S}(\boldsymbol{\omega})$ is the skew-symmetric matrix such that $\mathbf{S}(\boldsymbol{\omega})\boldsymbol{x}$ is the cross product $\boldsymbol{\omega} \times \boldsymbol{x}$. It is assumed that an Attitude and Heading Reference System (AHRS) installed on-board each agent provides measurements of both $\mathbf{R}_i(t)$ and $\boldsymbol{\omega}_i(t)$. Additionally, suppose that each agent has access to a linear acceleration measurement $\mathbf{a}_i(t) \in \mathbb{R}^3$, which follows

$$\mathbf{a}_i(t) = \dot{\mathbf{v}}_i(t) + \mathbf{S}(\boldsymbol{\omega}_i(t))\mathbf{v}_i(t) - \mathbf{g}_i(t), \tag{2}$$

where $\mathbf{g}_i(t) \in \mathbb{R}^3$ is the acceleration of gravity, expressed in body-fixed coordinates of the i-th agent. Even though the acceleration of gravity is usually well-known, it is treated as an unknown variable with practical applications in mind, where small errors in the estimation of the attitude of the agent may lead to significant errors in the acceleration compensation, see [21] for further details. Its time derivative is given by

$$\dot{\mathbf{g}}_i(t) = -\mathbf{S}(\boldsymbol{\omega}_i(t))\mathbf{g}_i(t). \tag{3}$$

For the first case, i.e., with inertial position readings, grouping equations (1) through (3), and measuring the inertial position, yields the system

$$\begin{cases} \dot{\mathbf{p}}_i(t) = \mathbf{R}_i(t)\mathbf{v}_i(t) \\ \dot{\mathbf{v}}_i(t) = -\mathbf{S}(\boldsymbol{\omega}_i(t))\mathbf{v}_i(t) + \mathbf{g}_i(t) + \mathbf{a}_i(t) \\ \dot{\mathbf{g}}_i(t) = -\mathbf{S}(\boldsymbol{\omega}_i(t))\mathbf{g}_i(t) \\ \mathbf{y}_i(t) = \mathbf{p}_i(t) \end{cases}.$$

Using in each vehicle the Lyapunov state transformation introduced in [22],

$$\begin{bmatrix} \mathbf{x}_i^1(t) \\ \mathbf{x}_i^2(t) \\ \mathbf{x}_i^3(t) \end{bmatrix} := \begin{bmatrix} \mathbf{I} & \mathbf{0} & \mathbf{0} \\ \mathbf{0} & \mathbf{R}_i(t) & \mathbf{0} \\ \mathbf{0} & \mathbf{0} & \mathbf{R}_i(t) \end{bmatrix} \begin{bmatrix} \mathbf{p}_i(t) \\ \mathbf{v}_i(t) \\ \mathbf{g}_i(t) \end{bmatrix}, \tag{4}$$

which preserves stability and observability properties [23], and making $\mathbf{u}_i(t) := \mathbf{R}_i(t)\mathbf{a}_i(t)$, the system dynamics can be written as the linear time-invariant (LTI) system

$$\begin{cases} \dot{\mathbf{x}}_i(t) = \mathbf{A}_L\mathbf{x}_i(t) + \mathbf{B}_L\mathbf{u}_i(t) \\ \mathbf{y}_i(t) = \mathbf{C}_L\mathbf{x}_i(t) \end{cases}, \tag{5}$$

where $\mathbf{x}_i^T(t) = \begin{bmatrix}[\mathbf{x}_i^1(t)]^T & [\mathbf{x}_i^2(t)]^T & [\mathbf{x}_i^3(t)]^T\end{bmatrix}^T \in \mathbb{R}^n$, $n = 9$, is the state of the system,

$$\mathbf{A}_L = \begin{bmatrix} \mathbf{0} & \mathbf{I} & \mathbf{0} \\ \mathbf{0} & \mathbf{0} & \mathbf{I} \\ \mathbf{0} & \mathbf{0} & \mathbf{0} \end{bmatrix} \in \mathbb{R}^{n\times n},\ \mathbf{B}_L = \begin{bmatrix} \mathbf{0} \\ \mathbf{I} \\ \mathbf{0} \end{bmatrix} \in \mathbb{R}^{n\times 3},$$

and $\mathbf{C}_L = \begin{bmatrix} \mathbf{I} & \mathbf{0} & \mathbf{0} \end{bmatrix} \in \mathbb{R}^{3\times n}$.

In the second case, i.e., when the agent has access to relative position measurements and receives position estimates from its source-agents, a similar procedure can be carried out. The relative position measurements of agent i are denoted by

$$\Delta\mathbf{p}_i(t) := \begin{bmatrix} \mathbf{p}_i(t) - \mathbf{p}_{a_{i,1}}(t) \\ \mathbf{p}_i(t) - \mathbf{p}_{a_{i,2}}(t) \\ \vdots \\ \mathbf{p}_i(t) - \mathbf{p}_{a_{i,N_i}}(t) \end{bmatrix} \in \mathbb{R}^{3N_i},\ a_{i,j} \in \mathcal{A}_i, \tag{6}$$

where

$$\mathcal{A}_i := \{a_{i,1}, a_{i,2}, \ldots, a_{i,N_i} |\, a_{i,j} \in \{1, \ldots, N\},\ j = 1, \ldots, N_i\}$$

is the set of source-agents of agent i and N_i is the number of source-agents of agent i. The position estimates received through communication with its source-agents are denoted by $\hat{\mathbf{p}}_{a_{i,j}}(t) \in \mathbb{R}^3$. Grouping equations (1) through (3) and taking the relative position measurements (6) as the output yields the system

$$\begin{cases} \dot{\mathbf{p}}_i(t) = \mathbf{R}_i(t)\mathbf{v}_i(t) \\ \dot{\mathbf{v}}_i(t) = -\mathbf{S}(\boldsymbol{\omega}_i(t))\mathbf{v}_i(t) + \mathbf{g}_i(t) + \mathbf{a}_i(t) \\ \dot{\mathbf{g}}_i(t) = -\mathbf{S}(\boldsymbol{\omega}_i(t))\mathbf{g}_i(t) \\ \mathbf{y}_i(t) = \Delta\mathbf{p}_i(t) \end{cases},$$

and applying (4) yields the compact form

$$\begin{cases} \dot{\mathbf{x}}_i(t) = \mathbf{A}_L\mathbf{x}_i(t) + \mathbf{B}_L\mathbf{u}_i(t) \\ \mathbf{y}_i(t) = \mathbf{C}_i\Delta\mathbf{x}_i(t) \end{cases}, \tag{7}$$

where $\mathbf{x}_i(t)$, $\mathbf{u}_i(t)$, $\mathbf{A}_L$, and $\mathbf{B}_L$ are defined as in (5), $\mathbf{C}_i = \mathbf{I}_{N_i} \otimes \mathbf{C}_L \in \mathbb{R}^{3N_i \times nN_i}$, and

$$\Delta\mathbf{x}_i(t) := \begin{bmatrix} \mathbf{x}_i(t) - \mathbf{x}_{a_{i,1}}(t) \\ \mathbf{x}_i(t) - \mathbf{x}_{a_{i,2}}(t) \\ \vdots \\ \mathbf{x}_i(t) - \mathbf{x}_{a_{i,N_i}}(t) \end{bmatrix} \in \mathbb{R}^{nN_i}.$$

The above system resembles the usual representation of LTI systems, the key difference being that the measurements on the system depend on some of the states of other agents.

2.2. Local Observers Dynamics

For the first case, simple calculations show that the pair $(\mathbf{A}_L, \mathbf{C}_L)$ is observable, thus it is straightforward to design a local state observer for agent i with globally asymptotically stable error dynamics [24].

For the second case, the dynamics of the local state observers are defined as

$$\begin{cases} \dot{\hat{\mathbf{x}}}_i(t) := \mathbf{A}_L\hat{\mathbf{x}}_i(t) + \mathbf{B}_L\mathbf{u}_i(t) + \mathbf{L}_i(\mathbf{y}_i(t) - \hat{\mathbf{y}}_i(t)) \\ \hat{\mathbf{y}}_i(t) := \mathbf{C}_i\Delta\hat{\mathbf{x}}_i(t) \end{cases}, \quad (8)$$

where $\hat{\mathbf{x}}_i(t) \in \mathbb{R}^n$ is the state estimate of agent i, $\mathbf{L}_i \in \mathbb{R}^{n \times 3N_i}$ is an arbitrary matrix of output feedback gains, to be determined, and

$$\Delta\hat{\mathbf{x}}_i(t) := \begin{bmatrix} \hat{\mathbf{x}}_i(t) - \hat{\mathbf{x}}_{a_{i,1}}(t) \\ \hat{\mathbf{x}}_i(t) - \hat{\mathbf{x}}_{a_{i,2}}(t) \\ \vdots \\ \hat{\mathbf{x}}_i(t) - \hat{\mathbf{x}}_{a_{i,N_i}}(t) \end{bmatrix} \in \mathbb{R}^{nN_i}.$$

Note that, due to the specific structure of $\mathbf{C}_i$, agent i only needs the position estimates $\hat{\mathbf{p}}_{a_{i,j}}(t)$ received from its source-agents to compute $\hat{\mathbf{y}}_i(t)$. Defining the state estimation error of agent i, $\tilde{\mathbf{x}}_i(t) \in \mathbb{R}^n$, as

$$\tilde{\mathbf{x}}_i(t) := \mathbf{x}_i(t) - \hat{\mathbf{x}}_i(t),$$

the state estimation error of its j-th source-agent $\tilde{\mathbf{x}}_{a_{i,j}}(t) \in \mathbb{R}^n$ as

$$\tilde{\mathbf{x}}_{a_{i,j}}(t) := \mathbf{x}_{a_{i,j}}(t) - \hat{\mathbf{x}}_{a_{i,j}}(t),$$

and splitting $\mathbf{L}_i$ into the blocks referring to each of the N_i distinct measurements,

$$\mathbf{L}_i = \begin{bmatrix} \mathbf{L}_i^{a_{i,1}} & \mathbf{L}_i^{a_{i,2}} & \dots & \mathbf{L}_i^{a_{i,N_i}} \end{bmatrix}, \mathbf{L}_i^{a_{i,j}} \in \mathbb{R}^{n \times 3},$$

the error dynamics can be written as

$$\dot{\tilde{\mathbf{x}}}_i(t) = \left(\mathbf{A}_L - \sum_{k=1}^{N_i} \mathbf{L}_i^{a_{i,k}} \mathbf{C}_L \right) \tilde{\mathbf{x}}_i(t) + \sum_{k=1}^{N_i} \mathbf{L}_i^{a_{i,k}} \mathbf{C}_L \tilde{\mathbf{x}}_{a_{i,k}}(t).$$

Remark 1. *It is possible to consider a third class of agents that would receive both absolute and relative position measurements. This is straightforward and therefore, for the sake of clarity of presentation, it is not considered in this work.*

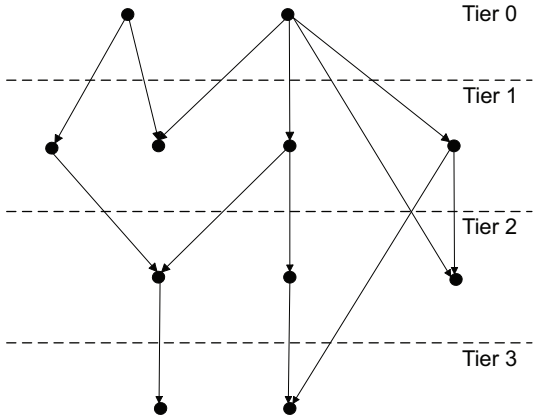

Figure 3: Drawing of an acyclic directed graph divided in tiers

Remark 2. *Note that the proposed decentralized arquitecture results in a much lower communication load in the formation when compared to centralized solutions. Denote the number of inertial and relative position measurements in the formation, respectively, by M_1 and M_2. In the centralized case, a central processing node will receive all $M_1 + M_2$ measurements from the agents, and in turn spread N position estimates through the formation. In the decentralized case, only M_2 position estimates need to be communicated, and they are all communicated through direct links between agents. Furthermore, the centralized solution will be much heavier computationally, as the central node will have to estimate N times as many state variables as a local state estimator.*

3. Stable Observer Gains

This section presents a design method for the decentralized state observer presented in the previous section that guarantees globally asymptotically stable error dynamics. Agent formations such as the one considered in this paper can be handily described by a directed graph, and as such it is convenient to introduce some concepts on graph theory [25, 26].

A directed graph, or digraph, $\mathcal{G} := (\mathcal{V}, \mathcal{E})$ is composed by a set $\mathcal{V}$ of vertices together with a set of directed edges $\mathcal{E}$, which are ordered pairs of vertices. Such an edge can be expressed as $e = (a, b)$, meaning that edge e is incident on vertices a and b, directed towards b. A directed path in $\mathcal{G}$ is a sequence $(v_0, e_1, v_1, e_2, v_2, \dots, e_n, v_n)$ of distinct vertices (with the possible exception of the first and the last) and edges of $\mathcal{G}$ such that $e_i = (v_{i-1}, v_i)$. A directed cycle is a directed path in which the first and the last vertices are the same. A directed graph is called acyclic if it contains no directed cycles.

If a directed graph $\mathcal{G}$ is acyclic, it can be represented graphically by a tiered drawing such as the one depicted in Fig. 3, that is, the drawing is divided in K hierarchical tiers following a few simple rules: tier 0 is composed of the vertices with no edges directed towards them while, for a vertex in tier $k > 0$, all directed paths ending in that vertex start in a node of a lower tier. In this paper, each vertex is denoted by its tier k and an identifier i in the respective tier (e.g., some quantity x associated

with vertex 4 in tier 2 is denoted as $x_{2/4}$, and the vertex itself is identified as $\{2/4\}$). Furthermore, the number of vertices in a given tier k is denoted by T_k.

Now, consider the agent formation described in the previous section. This kind of formation can be associated with a directed graph $\mathcal{G} = (\mathcal{V}, \mathcal{E})$, where each vertex represents a distinct agent, and an edge (a, b) means that agent a is a source-agent of agent b. Note that the vertices with no edges directed towards them refer to agents with access to measurements of their own absolute position.

The following result establishes a sufficient condition for global asymptotic stability of the estimation error for the distributed state observer.

Theorem 1. *Consider a formation composed of N agents, whose dynamics are described either by (5) or (7), depending on the type of measurements available to them, and assume that the digraph associated with the formation is acyclic. Suppose that each agent $\{a/b\}$ described by (5) implements a local state observer with globally asymptotically stable error dynamics, with gain $\mathbf{L}_{a/b} \in \mathbb{R}^{n\times 3}$, and that each agent $\{k/i\}$ described by (7) implements the local state observer (8), with the gain*

$$\mathbf{L}_{k/i} = \begin{bmatrix} \mathbf{L}_{k/i}^{a_{k/i,1}} & \mathbf{L}_{k/i}^{a_{k/i,2}} & \dots & \mathbf{L}_{k/i}^{a_{k/i,N_{k/i}}} \end{bmatrix}$$

chosen so that the matrix $\left(\mathbf{A}_L - \sum_{j=1}^{N_{k/i}} \mathbf{L}_{k/i}^{a_{k/i,j}} \mathbf{C}_L\right)$ is stable. Let $\tilde{\mathbf{x}}_{k/i} := \mathbf{x}_{k/i} - \hat{\mathbf{x}}_{k/i} \in \mathbb{R}^n$ denote the estimation error of each local observer in a tier, where k is its tier and $i \in \{1, 2, \dots, T_k\}$ corresponds to its identifier in the tier. Then, the estimation error of the distributed state observer,

$$\mathbf{e}(t) := \begin{bmatrix} \tilde{\mathbf{x}}_{0/1}(t) \\ \tilde{\mathbf{x}}_{0/2}(t) \\ \vdots \\ \tilde{\mathbf{x}}_{K-1/T_{K-1}}(t) \end{bmatrix} \in \mathbb{R}^{nN},$$

composed by the concatenation of the estimation error of each local observer, converges globally asymptotically to zero, and its dynamics satisfy

$$\dot{\mathbf{e}}(t) = \mathbf{\Lambda}\mathbf{e}(t), \tag{9}$$

for some $\mathbf{\Lambda} \in \mathbb{R}^{nN\times nN}$, whose eigenvalues are those of each local state observer.

Proof. Since the graph $\mathcal{G} = (\mathcal{V}, \mathcal{E})$ associated with the formation is acyclic, consider its drawing with K tiers each with T_k agents. Note that the dynamics of the local state observer of an agent in a given tier only depends on measurements from agents in lower tiers, allowing to study its properties regardless of the composition of higher tiers.

Since the agents in tier 0 have access to measurements of their absolute position, the global estimation error for that tier, $\mathbf{e}_0(t) := \begin{bmatrix}[\tilde{\mathbf{x}}_{0/1}(t)]^T & [\tilde{\mathbf{x}}_{0/2}(t)]^T & \dots & [\tilde{\mathbf{x}}_{0/T_0}(t)]^T\end{bmatrix}$ satisfies

$$\dot{\mathbf{e}}_0(t) = \mathbf{\Lambda}_0\mathbf{e}_0(t),$$

where

$$\mathbf{\Lambda}_0 = \text{diag}((\mathbf{A}_L - \mathbf{L}_{0/1}\mathbf{C}_L), \dots, (\mathbf{A}_L - \mathbf{L}_{0/T_0}\mathbf{C}_L))$$

is a stable matrix, by construction, whose eigenvalues are those of each local observer in tier 0.

Taking any tier $k > 0$, its error dynamics can be grouped with those of the lower tiers, yielding

$$\begin{bmatrix} \dot{\mathbf{e}}_{0,\dots,k-1}(t) \\ \dot{\mathbf{e}}_k(t) \end{bmatrix} = \begin{bmatrix} \mathbf{K} & \mathbf{0} \\ \mathbf{\Psi}_k & \mathbf{\Lambda}_k \end{bmatrix} \begin{bmatrix} \mathbf{e}_{0,\dots,k-1}(t) \\ \mathbf{e}_k(t) \end{bmatrix}, \tag{10}$$

where $\mathbf{K}$ is the matrix representing the estimation error dynamics of tiers 0 through $k-1$,

$$\Lambda_k = \text{diag}\left[\left(\mathbf{A}_L - \sum_{j=1}^{N_{k/1}} \mathbf{L}_{k/1}^{a_{k/1,j}} \mathbf{C}_L\right), \dots \right. \\ \left. \dots, \left(\mathbf{A}_L - \sum_{j=1}^{N_{k/T_k}} \mathbf{L}_{k/T_k}^{a_{k/T_k,j}} \mathbf{C}_L\right)\right]$$

is a stable matrix, by construction, whose eigenvalues are those of each local observer in tier k, and

$$\mathbf{\Psi}_k = \begin{bmatrix}[\mathbf{\Psi}_{k/1}]^T & [\mathbf{\Psi}_{k/2}]^T & \dots & [\mathbf{\Psi}_{k/T_k}]^T\end{bmatrix}^T,$$

where

$$\mathbf{\Psi}_{k/i} = \begin{bmatrix} \boldsymbol{\psi}_{k/i}(\{0/1\}) & \boldsymbol{\psi}_{k/i}(\{0/2\}) & \dots \\ & \dots & \boldsymbol{\psi}_{k/i}(\{k-1/T_{k-1}\}) \end{bmatrix}^T,$$

with

$$\boldsymbol{\psi}_{k/i}(\{a/b\}) = \begin{cases} \mathbf{L}_{k/i}^{a/b}\mathbf{C}_L, & \{a/b\} \in \mathcal{A}_{k/i} \\ \mathbf{0}, & \text{otherwise} \end{cases}.$$

From (10), it is straightforward to show that the eigenvalues of the global error dynamics of tiers 0 through k are those of $\mathbf{K}$ and $\mathbf{\Lambda}_k$. Therefore, if the matrix representing the dynamics of the global estimation error of tiers 0 to $k-1$, $\mathbf{K}$, is stable, then the dynamics of the global estimation error of tiers 0 to k will also be stable, and the error will converge globally asymptotically to zero. Since:

1) the distributed state estimator formed by all agents in tier 0 is stable, and the eigenvalues of the dynamics of its estimation error are those of each local observer in tier 0, and

2) the addition of tier k to the dynamics of the estimation error of the previous tiers yields new error dynamics whose eigenvalues are those of the previous tiers, plus the eigenvalues of the error dynamics of each state observer in tier k, it follows, by induction, that the dynamics of the global estimation error of the full formation satisfy (9), where the eigenvalues of $\mathbf{\Lambda}$ are those of each local observer. Moreover, since the matrix $\mathbf{L}_{k/i}$ of each state observer is chosen such that $\left(\mathbf{A}_L - \sum_{j=1}^{N_{k/i}} \mathbf{L}_{k/i}^{a_{k/i,j}} \mathbf{C}_L\right)$ is stable, the estimation error converges globally asymptotically to zero. □

This result allows the design of a distributed estimator in the terms described in Section 2. Note that the state observer of each agent can be designed locally and results from the solution of simple stable pole placement problems.

Remark 3. *It is also possible to use this method to design a stable state observer when there are cycles in the graph $\mathcal{G}$ associated with the formation by removing edges from the graph until it is no longer cyclic, while making sure to never remove the last edge directed towards a vertex. It seems naturally advantageous to remove as few edges as possible, therefore this procedure could be restated as that of finding the maximum acyclic subgraph of $\mathcal{G}$ [27], with the added restriction that the last edge directed towards a vertex may not be removed. This straightforward approach is then applied to the observers by zeroing the gains referring to edges which were removed during this process but that are actually available for observer design purposes.*

4. Performance in Noisy Environments

The previous section presented a method for designing decentralized state observers for agent formations such as the one described in Section 2. While stability is assured, there are no guarantees regarding performance in noisy environments, which is critical in most practical settings. As such, this section introduces a method for improving the performance of the state observer in the presence of sensor noise which, in addition, naturally admits the presence of cycles in the formation graph.

4.1. Global Observer Dynamics

To study and improve the performance of the decentralized state observer, it is necessary to consider the global dynamics of the formation, which can be represented in the LTI form

$$\begin{cases} \dot{\boldsymbol{x}}(t) = \mathbf{A}_g \boldsymbol{x}(t) + \mathbf{B}_g \boldsymbol{u}(t) + \mathbf{w}(t) \\ \boldsymbol{y}(t) = \mathbf{C}_g \boldsymbol{x}(t) + \mathbf{v}(t) \end{cases}, \tag{11}$$

where $\boldsymbol{x}(t) := \begin{bmatrix} \mathbf{x}_1^T(t) & \dots & \mathbf{x}_N^T(t) \end{bmatrix}^T \in \mathbb{R}^{nN}$ is the state of the whole formation, $\boldsymbol{y}(t) := \begin{bmatrix} \mathbf{y}_1^T(t) & \dots & \mathbf{y}_N^T(t) \end{bmatrix}^T \in \mathbb{R}^{3M}$ the output of the system, M being the total number of absolute and relative position measurements in the whole formation, and $\boldsymbol{u}(t) := \begin{bmatrix} \mathbf{u}_1^T(t) & \dots & \mathbf{u}_N^T(t) \end{bmatrix}^T \in \mathbb{R}^{3N}$ is the input of the system. The variables $\mathbf{w}(t) \in \mathbb{R}^{nN}$ and $\mathbf{v}(t) \in \mathbb{R}^{3M}$ represent, respectively, process and observation noise, which are assumed to be zero-mean uncorrelated white Gaussian processes, with associated covariance matrices $\boldsymbol{\Xi} \in \mathbb{R}^{nN \times nN}$ and $\boldsymbol{\Theta} \in \mathbb{R}^{3M \times 3M}$. The matrices $\mathbf{A}_g \in \mathbb{R}^{nN \times nN}$ and $\mathbf{B}_g \in \mathbb{R}^{nN \times 3N}$ are built from the dynamics of the individual agents, following

$$\begin{cases} \mathbf{A}_g = \mathbf{I}_N \otimes \mathbf{A}_L \\ \mathbf{B}_g = \mathbf{I}_N \otimes \mathbf{B}_L \end{cases}.$$

To describe $\mathbf{C}_g \in \mathbb{R}^{3M \times nN}$, it is useful to build a matrix $\mathbf{S} \in \mathbb{R}^{N \times M}$ similar to the incidence matrix of graph $\mathcal{G}$. First, define virtual edges of the form $(0, i)$ to represent the absolute position measurements that are available to some of the agents, then build $\mathbf{S}$ the same way the incidence matrix would be built, that is, its individual entries follow

$$\mathbf{S}_{ij} = \begin{cases} 1, & \text{edge } j \text{ incident on } i, \text{ directed towards it,} \\ -1, & \text{edge } j \text{ incident on } i, \text{ directed away from it,} \\ 0, & \text{otherwise.} \end{cases}$$

Then, $\mathbf{C}_g$ follows

$$\mathbf{C}_g = \mathbf{S}^T \otimes \mathbf{C}_L.$$

The local state observers can also be grouped in a similar way, yielding

$$\begin{cases} \dot{\hat{\boldsymbol{x}}}(t) := \mathbf{A}_g \hat{\boldsymbol{x}}(t) + \mathbf{B}_g \boldsymbol{u}(t) + \mathbf{L}(\boldsymbol{y}(t) - \hat{\boldsymbol{y}}(t)) \\ \hat{\boldsymbol{y}}(t) := \mathbf{C}_g \hat{\boldsymbol{x}}(t) \end{cases}, \tag{12}$$

where $\hat{\boldsymbol{x}}(t) := \begin{bmatrix} \hat{\mathbf{x}}_1^T(t) & \hat{\mathbf{x}}_2^T(t) & \dots & \hat{\mathbf{x}}_N^T(t) \end{bmatrix}^T \in \mathbb{R}^{nN}$ is the global state estimate of the decentralized state observer, and $\mathbf{L} \in \mathbb{R}^{nN \times 3M}$ is the matrix of observer gains. To account for the fact that each local observer only has access to some measurements, $\mathbf{L}$ must follow a special structure, or sparsity constraint. More specifically, define an augmented incidence matrix, $\mathbf{S}' \in \mathbb{R}^{nN \times 3M}$, as

$$\mathbf{S}' = \mathbf{S} \otimes \mathbf{1}_{n,3},$$

where $\mathbf{1}_{n,m}$ is a $n \times m$ matrix whose entries are all equal to 1. Then, the individual entries of $\mathbf{L}$ follow

$$\begin{cases} \mathbf{S}'_{ij} = 1 \Rightarrow \mathbf{L}_{ij} \text{ can be set to an arbitrary value} \\ \mathbf{S}'_{ij} \neq 1 \Rightarrow \mathbf{L}_{ij} = 0. \end{cases}$$

This can be expressed as linear constraint for optimization purposes:

$$\begin{aligned} \mathbf{L}_{ij} = 0 \quad & \text{if} \quad \mathbf{S}'_{ij} \neq 1, \\ & \forall i \in \{1, 2, \dots, nN\},\ j \in \{1, 2, \dots, 3M\}. \end{aligned} \tag{13}$$

The sparsity constraint imposed on $\mathbf{L}$ prevents the use of classical filter design techniques such as the Kalman filter, and as such a different strategy must be pursued to find suitable observer gains.

4.2. H_2 Nominal Performance

Consider the system

$$\begin{cases} \dot{\mathbf{x}}(t) = \mathbf{A}\mathbf{x}(t) + \mathbf{B}\mathbf{u}(t) \\ \mathbf{z}(t) = \mathbf{C}\mathbf{x}(t) + \mathbf{D}\mathbf{u}(t) \end{cases}, \tag{14}$$

where $\mathbf{x}(t) \in \mathbb{R}^m$ is the state of the system, $\mathbf{u}(t) \in \mathbb{R}^o$ the input, and $\mathbf{z}(t) \in \mathbb{R}^p$ is the output. The matrices $\mathbf{A}$, $\mathbf{B}$, $\mathbf{C}$, and $\mathbf{D}$ are constant real matrices of appropriate dimensions. Denote the corresponding transfer function by $\mathbf{T}(s) = \mathbf{C}(\mathbf{I}s - \mathbf{A})^{-1}\mathbf{B} + \mathbf{D}$.

The H_2 norm of the system, $\|\mathbf{T}\|_{H_2}$, which verifies

$$\|\mathbf{T}\|_{H_2}^2 = \frac{1}{2\pi} \text{trace} \int_{-\infty}^{\infty} \mathbf{T}(j\omega)\mathbf{T}(j\omega)^* d\omega,$$

can be used as a performance metric for state observers. In fact, when the components of the input $\mathbf{u}(t)$ are independent zero-mean, white Gaussian noise processes, the H_2 norm of the system is also the asymptotic output variance of the system [28]. The global error of the decentralized state observer (12), $\tilde{\boldsymbol{x}}(t) \in \mathbb{R}^{nN}$, is defined as

$$\tilde{\boldsymbol{x}}(t) = \boldsymbol{x}(t) - \hat{\boldsymbol{x}}(t).$$

Taking its time derivative and using (11) and (12) yields

$$\dot{\tilde{\boldsymbol{x}}}(t) = (\mathbf{A}_g - \mathbf{L}\mathbf{C}_g)\tilde{\boldsymbol{x}}(t) + \mathbf{w}(t) - \mathbf{L}\mathbf{v}(t). \tag{15}$$

Define a zero-mean, uncorrelated, white Gaussian noise process $\mathbf{q}(t) \in \mathbb{R}^{nN+3M}$ whose covariance is the identity matrix. The error dynamics (15) can then be rewritten as

$$\dot{\tilde{\boldsymbol{x}}}(t) = (\mathbf{A}_g - \mathbf{L}\mathbf{C}_g)\tilde{\boldsymbol{x}}(t) + \begin{bmatrix}\boldsymbol{\Xi}^{\frac{1}{2}} & -\mathbf{L}\boldsymbol{\Theta}^{\frac{1}{2}}\end{bmatrix}\mathbf{q}(t).$$

By making the substitution

$$\begin{cases} \mathbf{A} = \mathbf{A}_g - \mathbf{L}\mathbf{C}_g \\ \mathbf{B} = \begin{bmatrix}\boldsymbol{\Xi}^{\frac{1}{2}} & -\mathbf{L}\boldsymbol{\Theta}^{\frac{1}{2}}\end{bmatrix} \\ \mathbf{C} = \mathbf{I} \\ \mathbf{D} = \mathbf{0} \\ \mathbf{x}(t) = \tilde{\boldsymbol{x}}(t) \\ \mathbf{u}(t) = \mathbf{q}(t) \end{cases}, \tag{16}$$

the system (14) describes the error dynamics of the decentralized state observer, and its H_2 norm is also the asymptotic variance of the estimation error. Thus, the problem of optimizing the performance of the state observer in noisy environments can be restated as minimizing the H_2 norm of (14), where the system state, output, and matrices are given by (16).

Consider the following result, resorting to Linear Matrix Inequality (LMI) concepts, as described in [28], presented here in a simplified form:

Theorem 2. *Suppose that the system (14) is asymptotically stable. Then*

1. $\|\mathbf{T}\|_2 < \infty$ *if and only if* $\mathbf{D} = \mathbf{0}$.
2. *If* $\mathbf{D} = 0$ *then the following statements are equivalent:*
   (a) $\|\mathbf{T}\|_2 < \gamma$.
   (b) *there exists* $\mathbf{P} = \mathbf{P}^T \succ \mathbf{0}$ *and* $\mathbf{Z}$ *such that*

$$\begin{bmatrix}\mathbf{A}^T\mathbf{P} + \mathbf{P}\mathbf{A} & \mathbf{P}\mathbf{B} \\ \mathbf{B}^T\mathbf{P} & -\gamma\mathbf{I}\end{bmatrix} \prec \mathbf{0}, \begin{bmatrix}\mathbf{P} & \mathbf{C}^T \\ \mathbf{C} & \mathbf{Z}\end{bmatrix} \succ \mathbf{0},$$

   and $trace(\mathbf{Z}) < \gamma$.

Define

$$\mathbf{X}(\mathbf{P}, \mathbf{L}, \gamma) := \begin{bmatrix}(\mathbf{A}_g - \mathbf{L}\mathbf{C}_g)^T\mathbf{P} + \mathbf{P}(\mathbf{A}_g - \mathbf{L}\mathbf{C}_g) & \mathbf{P}\begin{bmatrix}\boldsymbol{\Xi}^{\frac{1}{2}} & -\mathbf{L}\boldsymbol{\Theta}^{\frac{1}{2}}\end{bmatrix} \\ \begin{bmatrix}\boldsymbol{\Xi}^{\frac{1}{2}} & -\mathbf{L}\boldsymbol{\Theta}^{\frac{1}{2}}\end{bmatrix}^T\mathbf{P} & -\gamma\mathbf{I}\end{bmatrix}$$

Using Theorem 2 and the substitution (16), the minimization of the H_2 norm of (14) considering the constraints (13) imposed by the graph topology can be done solving the optimization problem [28]

$$\begin{aligned} \min_{\substack{\mathbf{P} \in \mathbb{R}^{nN\times nN} \\ \mathbf{L} \in \mathbb{R}^{nN\times 3M} \\ \mathbf{Z} \in \mathbb{R}^{nN\times nN} \\ \gamma \in \mathbb{R}^+}} \quad & \gamma \\ \text{subject to:} \quad & \mathbf{P} \succ \mathbf{0}, \\ & \mathbf{X}(\mathbf{P}, \mathbf{L}, \gamma) \prec 0, \\ & \begin{bmatrix}\mathbf{P} & \mathbf{I} \\ \mathbf{I} & \mathbf{Z}\end{bmatrix} \succ \mathbf{0}, \\ & \text{trace}(\mathbf{Z}) < \gamma, \\ & \text{and } \mathbf{L}_{ij} = 0 \text{ if } \mathbf{S}'_{ij} \neq 1, \\ & \forall i \in \{1, 2, \ldots, nN\}, j \in \{1, 2, \ldots, 3M\}. \end{aligned} \tag{17}$$

The resulting set of constraints contains a BMI, which is inherently difficult to treat and is usually associated with nonconvex problems. In fact, even finding a feasible solution is a NP-hard problem [29]. While it is possible, for centralized systems, to apply a variable substitution which renders the constraints linear, the structural constraint imposed on $\mathbf{L}$ in the decentralized case inviabilizes this approach. On the other hand, Theorem 1 allows to find stable observer gains, and as such provides a way to find a feasible set of variables for the constraints of (17). In fact, if the value of $\mathbf{L}$ is fixed, the constraints take a Linear Matrix Inequality (LMI) form, and there exist very fast and efficient methods to solve optimization problems with LMI constraints. Following this, Table 1 details an algorithm for improvement of the performance of the decentralized state observer, similar to the $\mathcal{P} - \mathcal{K}$ iterations used in some cases for controller design via BMIs [18].

Note that there are no guarantees that the algorithm will find the optimal observer gains, or even that it will improve on the initial $\mathbf{L}$. However, there is the guarantee that γ is non-increasing. In step 2 of the k-th iteration of the algorithm, solving (18) yields optimal γ and $\mathbf{P}^{(k)}$ for the given $\mathbf{L}^{(k-1)}$. Denote the values found for $\mathbf{Z}$ and γ, respectively, by $\mathbf{Z}^*$ and γ^*. Then, in step 3, the constraints of (19) will have at least one feasible set of variables for which $\gamma \leq \gamma^*$: $(\mathbf{L}^{(k-1)}, \mathbf{Z}^*, \gamma^*)$. The same reasoning can be applied to show that the value of γ computed in (18) is, at most, the value of γ found in step 3 of the previous iteration and, as such, γ is non-increasing over the run of the algorithm.

5. Further extensions

This section briefly details possible extensions of the results presented in the previous sections, and is divided in two parts: in the first, an alternative mission scenario is considered, while the second part describes a method to obtain H_∞ norm performance guarantees for the global estimation error of the formation.

5.1. Extension to alternative scenarios

The aim of this subsection is to demonstrate the possibility of applying the results of Sections 3 and 4 to alternative cases that differ from the mission scenario described in Section 2. More specifically, this subsection explores the alternative scenario in

Table 1: Algorithm for H_2 norm minimization

1) Initialization: set $k = 1$; find $\mathbf{L}^{(0)}$ such that $(\mathbf{A}_g - \mathbf{L}^{(0)}\mathbf{C}_g)$ is stable (this can be done following, e.g., Theorem 1); choose a stopping criterion for the algorithm (e.g. a fixed number of steps, or a minimum improvement on the value of γ at each iteration).
2) Solve the optimization problem with LMI constraints

$$\begin{aligned} \min_{\substack{\mathbf{P}^{(k)} \in \mathbb{R}^{nN\times nN} \\ \mathbf{Z} \in \mathbb{R}^{nN\times nN} \\ \gamma \in \mathbb{R}^{+}}} \quad & \gamma \\ \text{subject to:} \quad & \mathbf{P}^{(k)} \succ \mathbf{0}, \\ & \mathbf{X}(\mathbf{P}^{(k)}, \mathbf{L}^{(k-1)}, \gamma) \prec 0, \\ & \begin{bmatrix} \mathbf{P}^{(k)} & \mathbf{I} \\ \mathbf{I} & \mathbf{Z} \end{bmatrix} \succ \mathbf{0}, \\ & \text{and } \mathrm{trace}(\mathbf{Z}) < \gamma. \end{aligned} \tag{18}$$

3) Solve the optimization problem with LMI constraints

$$\begin{aligned} \min_{\substack{\mathbf{L}^{(k)} \in \mathbb{R}^{nN\times 3M} \\ \mathbf{Z} \in \mathbb{R}^{nN\times nN} \\ \gamma \in \mathbb{R}^{+}}} \quad & \gamma \\ \text{subject to:} \quad & \mathbf{X}(\mathbf{P}^{(k)}, \mathbf{L}^{(k)}, \gamma) \prec 0, \\ & \begin{bmatrix} \mathbf{P}^{(k)} & \mathbf{I} \\ \mathbf{I} & \mathbf{Z} \end{bmatrix} \succ \mathbf{0}, \\ & \mathrm{trace}(\mathbf{Z}) < \gamma, \\ & \text{and } \mathbf{L}_{ij}^{(k)} = 0 \text{ if } \mathbf{S}'_{ij} \neq 1, \ \forall i, j. \end{aligned} \tag{19}$$

4) If the stopping criterion is met, stop and take $\mathbf{L}^{(k)}$ as the gain for the decentralized state observer. Otherwise, set $k = k + 1$ and go to step 2.

which the agents in the formation are operating in the presence of a constant unknown current, and have mounted on-board a Doppler Velocity Log (DVL) instead of an accelerometer.

In this case, the DVL provides the velocity of the agent relative to the fluid, therefore it is convenient to divide the velocity of each agent, $\mathbf{v}_i(t)$, in two components: the velocity of the agent relative to the fluid, $\mathbf{v}_{ri}(t) \in \mathbb{R}^3$, measured in body-fixed coordinates, and the velocity of the fluid relative to $\{\mathrm{I}\}$, $\mathbf{v}_{fi}(t) \in \mathbb{R}^3$, also expressed in body-fixed coordinates. Thus, (1) can be rewritten as

$$\dot{\mathbf{p}}_i(t) = \mathbf{R}_i(t)(\mathbf{v}_{ri}(t) + \mathbf{v}_{fi}(t)),$$

with

$$\dot{\mathbf{v}}_{fi}(t) = -\mathbf{S}(\boldsymbol{\omega}_i(t))\mathbf{v}_{fi}(t).$$

Define a coordinate transformation

$$\mathbf{T}_{i2}(t) = \begin{bmatrix} \mathbf{I} & \mathbf{0} \\ \mathbf{0} & \mathbf{R}_i(t) \end{bmatrix},$$

which is a Lyapunov state transformation, and define new state variables

$$\boldsymbol{\chi}_i(t) = \begin{bmatrix} \boldsymbol{\chi}_i^1(t) \\ \boldsymbol{\chi}_i^2(t) \end{bmatrix} = \mathbf{T}_{i2}(t) \begin{bmatrix} \mathbf{p}_i(t) \\ \mathbf{v}_{fi}(t) \end{bmatrix} \in \mathbb{R}^6.$$

Taking as outputs the relative position measurements (6) yields the dynamic system

$$\begin{cases} \dot{\boldsymbol{\chi}}_i(t) = \mathbf{A}_{L2}\boldsymbol{\chi}_i(t) + \mathbf{B}_{L2}\boldsymbol{\mu}_i(t) \\ \mathbf{y}_i(t) = \mathbf{C}_{i2}\Delta\boldsymbol{\chi}_i(t) \end{cases}, \tag{20}$$

where

$$\mathbf{A}_{L2} = \begin{bmatrix} \mathbf{0} & \mathbf{I} \\ \mathbf{0} & \mathbf{0} \end{bmatrix} \in \mathbb{R}^{6\times 6}, \ \mathbf{B}_{L2} = \begin{bmatrix} \mathbf{I} \\ \mathbf{0} \end{bmatrix} \in \mathbb{R}^{6\times 3},$$

$$\mathbf{C}_{i2} = \begin{bmatrix} \mathbf{I} & \mathbf{0} \\ \vdots & \vdots \\ \mathbf{I} & \mathbf{0} \end{bmatrix} \in \mathbb{R}^{3N_i\times 6},$$

$$\Delta\boldsymbol{\chi}_i(t) := \begin{bmatrix} \boldsymbol{\chi}_i(t) - \boldsymbol{\chi}_{a_{i,1}}(t) \\ \boldsymbol{\chi}_i(t) - \boldsymbol{\chi}_{a_{i,2}}(t) \\ \vdots \\ \boldsymbol{\chi}_i(t) - \boldsymbol{\chi}_{a_{i,N_i}}(t) \end{bmatrix} \in \mathbb{R}^{6N_i}, \ a_{i,j} \in \mathcal{A}_i,$$

and $\boldsymbol{\mu}_i(t) = \mathbf{R}_i(t)\mathbf{v}_{ri}(t)$. Following this, it is straightforward to show that the results derived in Sections 3 and 4 can also be applied when the local dynamics of the agents in the formation are described by (20).

5.2. H_∞ norm minimization

The H_2 norm minimization process detailed in Section 4 is not the only way of improving the performance of the decentralized state estimator in the presence of measurement noise. A possible alternative is to minimize the H_∞ norm of the global estimation error instead of its H_2 norm. Consider the following result from [28], presented here in a simplified form:

Theorem 3. *Suppose that the system (14) is asymptotically stable, and $\gamma > 0$. Then, the following statements are equivalent:*

1. $\|\mathbf{T}\|_\infty < \gamma$.
2. *For all* $\mathbf{u}$ *there holds that*

$$\sup_{0<\|\mathbf{u}\|_2<\infty} \frac{\|\mathbf{z}\|_2}{\|\mathbf{u}\|_2} < \gamma,$$

   where $\mathbf{z}$ *is the output of (14) subject to input* $\mathbf{u}$ *and initial condition* $\mathbf{x}(0) = 0$.
3. *There exists a solution* $\mathbf{K} = \mathbf{K}^T \succ \mathbf{0}$ *to the LMI*

$$\begin{bmatrix} \mathbf{A}^T\mathbf{K} + \mathbf{K}\mathbf{A} + \mathbf{C}^T\mathbf{C} & \mathbf{K}\mathbf{B} + \mathbf{C}^T\mathbf{D} \\ \mathbf{B}^T\mathbf{K} + \mathbf{D}^T\mathbf{C} & \mathbf{D}^T\mathbf{D} - \gamma^2\mathbf{I} \end{bmatrix} \prec \mathbf{0}.$$

By making the substitution

$$\begin{cases} \mathbf{A} = \mathbf{A}_g - \mathbf{L}\mathbf{C}_g \\ \mathbf{B} = \begin{bmatrix} \mathbf{I} & -\mathbf{L} \end{bmatrix} \\ \mathbf{C} = \mathbf{I} \\ \mathbf{D} = \mathbf{0} \\ \mathbf{x}(t) = \tilde{\boldsymbol{x}}(t) \\ \mathbf{u}(t) = \begin{bmatrix} \mathbf{w}(t) \\ \mathbf{v}(t) \end{bmatrix} \end{cases},$$

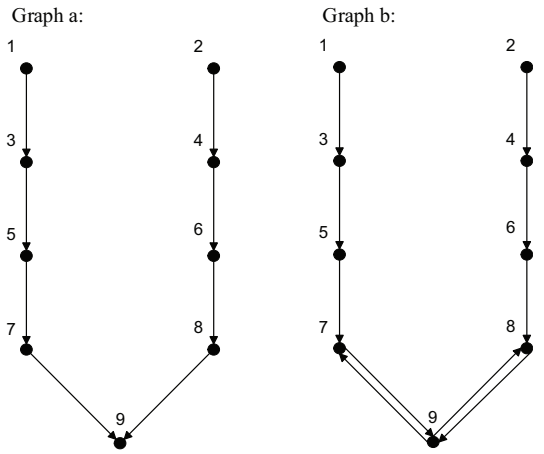

Figure 4: Digraphs associated with the agent formations considered in simulation

it follows that the observer gains that minimize the H_∞ norm of the global estimation error are given by the solution of the following optimization problem with BMI constraints:

$$\begin{aligned} \min_{\substack{\mathbf{K}\in\mathbb{R}^{nN\times nN}\\ \mathbf{L}\in\mathbb{R}^{nN\times 3M}\\ \gamma\in\mathbb{R}^{+}}} \quad & \gamma \\ \text{subject to:} \quad & \mathbf{K}\succ\mathbf{0}, \\ & \mathbf{X}_\infty(\mathbf{K},\mathbf{L},\gamma)\prec 0, \\ & \text{and } \mathbf{L}_{ij}=0 \text{ if } \mathbf{S}'_{ij}\neq 1, \\ & \forall i\in\{1,2,\ldots,nN\}, j\in\{1,2,\ldots,3M\}. \end{aligned},$$

where

$$\mathbf{X}_\infty(\mathbf{K},\mathbf{L},\gamma) := \begin{bmatrix} (\mathbf{A}_g-\mathbf{L}\mathbf{C}_g)^T\mathbf{K}+\mathbf{K}(\mathbf{A}_g-\mathbf{L}\mathbf{C}_g)+\mathbf{I} & \mathbf{K}\begin{bmatrix}\mathbf{I} & -\mathbf{L}\end{bmatrix} \\ \begin{bmatrix}\mathbf{I} & -\mathbf{L}\end{bmatrix}^T\mathbf{K} & -\gamma^2\mathbf{I} \end{bmatrix}.$$

6. Simulation Results

This section presents the results of simulations that were carried out in order to assess the performance of the proposed decentralized state observers. Two similar formation structures were considered, with associated graphs depicted in Fig. 4. The key difference between both is that, while graph (a) is acyclic, graph (b) has two additional edges that render it cyclic. The results are divided in two parts. In the first one, the algorithm proposed in the previous section is used for the two different formation structures, using in each case several distinct initial values for $\mathbf{L}$, which were found using Theorem 1. The second part takes the best gain $\mathbf{L}$ found for each formation structure and compares their performance in simulation.

6.1. H_2 Norm Minimization

To optimize the state observer gains, the process and observation noise must first be characterized. In the simulations, the linear acceleration and relative position measurements were corrupted by additive, uncorrelated, zero-mean white Gaussian

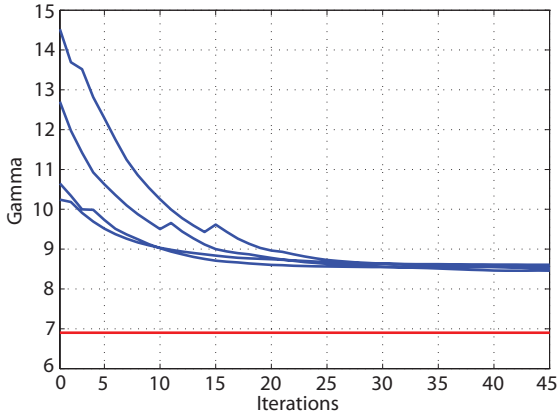

Figure 5: Evolution of the algorithm for different initial conditions, acyclic graph. In red, H_2 norm of the centralized filter

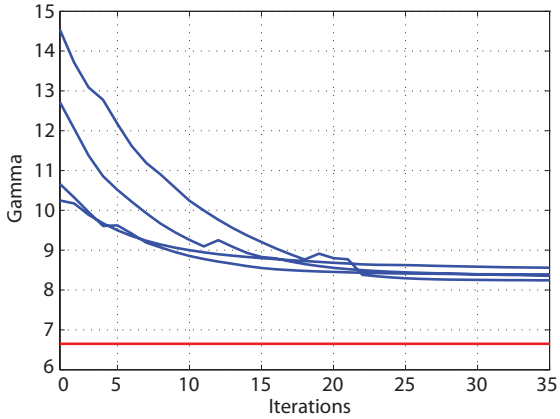

Figure 6: Evolution of the algorithm for different initial conditions, cyclic graph. In red, H_2 norm of the centralized filter

noise, with standard deviations of $0.01\ (\mathrm{m/s^2})$ and $1\ (\mathrm{m})$, respectively. Assuming that the two AUVs with access to absolute position measurements do so by implementing a LBL or USBL positioning system and share the same set of landmarks, some correlation in the noise of those measurements is to be expected. Thus, the absolute position measurements were corrupted by additive, zero-mean white Gaussian noise with standard deviation of $0.1\ (\mathrm{m})$, and some correlation between the two measurements was added, resulting in the following covariance matrix:

$$\mathbf{\Theta}_0 = 0.01\times\begin{bmatrix}1 & 0.1\\ 0.1 & 1\end{bmatrix}\otimes\mathbf{I}_3.$$

Following this, $\mathbf{\Xi}$ and $\mathbf{\Theta}$ were set to

$$\begin{cases} \mathbf{\Xi} = \mathrm{diag}\left(0.0001,\ 0.0001,\ \ldots,\ 0.0001\right) \\ \mathbf{\Theta} = \mathrm{diag}\left(\mathbf{\Theta}_0,\ \mathbf{\Theta}_1,\ \mathbf{\Theta}_1,\ \ldots,\ \mathbf{\Theta}_1\right) \end{cases},$$

where $\mathbf{\Theta}_0$ refers to the absolute position measurements of agents 1 and 2, while $\mathbf{\Theta}_1 = \mathbf{I}$ refers to the relative position measurements available to the other agents.

The evolution of the H_2 cost during the optimization algorithm for the acyclic and cyclic graph is depicted in Fig. 5 and

Table 2: Lowest value achieved for γ

	Acy./Decent.	Acy./Cent.	Cyc./Decent.	Cyc./Cent.
γ_{min}	8.458	6.902	8.242	6.649

Fig. 6, respectively, with 4 distinct initial values of $\mathbf{L}$. The lines in red represent the H_2 norm of the optimal centralized filter, whose gains were computed using classical Kalman filtering theory, see [30]. To complement the graphical data, Table 2 details the best values found in each case, and also the H_2 norm of the optimal centralized filter, to provide a comparison term. The results show that, in every case, the algorithm improved on the initial $\mathbf{L}$ and that, in the cyclic case, it used the additional edges constructively and it achieved better values than in the acyclic one. Note that, in the decentralized case, the agents have access to only a small fraction of the total number of measurements in the whole formation, so it would be unreasonable to expect the decentralized state observer to attain the performance of the optimal centralized one. Nevertheless, the performances that are achieved with the distributed solutions are very good considering the overwhelming communication and computational costs of the centralized filter.

Remark 4. *As it was discussed in the previous section, theoretically, the value of γ is non-increasing over the run of the algorithm. However, Fig. 5 and Fig. 6 show a few outliers where the H_2 norm increases. This is due to numerical errors in the solvers used to find solutions for (18) and (19).*

6.2. Performance assessment and comparison

The simulations were carried out for four different state estimators:

1. A decentralized state estimator based on the acyclic formation graph (Figure 4, graph a), with the best gains found through the application of the proposed H_2 norm minimization algorithm.
2. A decentralized state estimator based on the cyclic formation graph (Figure 4, graph b), with the best gains found through the application of the proposed H_2 norm minimization algorithm.
3. A centralized Kalman filter based on the cyclic formation graph, to provide a lower bound for the attainable performance.
4. A decentralized estimator using gains obtained by straightforward application of Theorem 1. In this case, one of the gains computed to provide initial values for the H_2 minimization algorithm was used.

The local state observers were implemented in the body-fixed coordinate frame of their respective agents. To do so, define new state estimates in the body-fixed coordinate frame, $\hat{\mathbf{z}}_i(t) \in \mathbb{R}^n$, by applying the inverse of the transformation used in (4), that is,

$$\hat{\mathbf{z}}_i(t) := \begin{bmatrix} \hat{\mathbf{p}}_i(t) \\ \hat{\mathbf{v}}_i(t) \\ \hat{\mathbf{g}}_i(t) \end{bmatrix} = \mathbf{T}_i^T(t)\hat{\mathbf{x}}_i(t),$$

where

$$\mathbf{T}_i(t) = \begin{bmatrix} \mathbf{I} & \mathbf{0} & \mathbf{0} \\ \mathbf{0} & \mathbf{R}_i(t) & \mathbf{0} \\ \mathbf{0} & \mathbf{0} & \mathbf{R}_i(t) \end{bmatrix} \in \mathbb{R}^{n\times n}. \tag{21}$$

By computing the time derivative of $\mathbf{z}_i(t)$, it follows that the corresponding state estimator in the body-fixed coordinate frame takes the form

$$\begin{cases} \dot{\hat{\mathbf{z}}}_i(t) = \mathbf{A}_i(t)\hat{\mathbf{z}}_i(t) + \mathbf{B}_L\mathbf{a}_i(t) + \mathbf{T}_i^T(t)\mathbf{L}_i(\mathbf{y}_i(t) - \hat{\mathbf{y}}_i(t)) \\ \hat{\mathbf{y}}_i(t) = \mathbf{C}_i\Delta\hat{\mathbf{z}}_i(t) \end{cases},$$

where $\mathbf{B}_L$, $\mathbf{C}_i$, and $\mathbf{a}_i(t)$ are defined as in Section 2, $\mathbf{L}_i$ is the output injection matrix of the local state observer designed in the inertial coordinate frame,

$$\Delta\hat{\mathbf{z}}_i(t) := \begin{bmatrix} \hat{\mathbf{z}}_i(t) - \hat{\mathbf{z}}_{a_{i,1}}(t) \\ \hat{\mathbf{z}}_i(t) - \hat{\mathbf{z}}_{a_{i,2}}(t) \\ \vdots \\ \hat{\mathbf{z}}_i(t) - \hat{\mathbf{z}}_{a_{i,N_i}}(t) \end{bmatrix} \in \mathbb{R}^{nN_i}, a_{i,j} \in \mathcal{A}_i,$$

where $\mathcal{A}_i$ is defined as in (6), and

$$\mathbf{A}_i(t) = \begin{bmatrix} \mathbf{0} & \mathbf{R}_i(t) & \mathbf{0} \\ \mathbf{0} & -\mathbf{S}(\boldsymbol{\omega}_i(t)) & \mathbf{I} \\ \mathbf{0} & \mathbf{0} & -\mathbf{S}(\boldsymbol{\omega}_i(t)) \end{bmatrix} \in \mathbb{R}^{n\times n}.$$

Note that, as (21) is a Lyapunov state transformation, it follows that these new local state estimators retain the convergence and stability properties of their counterparts fully designed in the inertial reference frame. Furthermore, the resulting global state estimator is also related to the one in inertial coordinates through a Lyapunov state transformation, thus retaining global stability properties.

In addition to the noise in the position and acceleration measurements, noise was also simulated in the attitude and angular velocity measurements required for the implementation of the local state observers in the original coordinated space, as provided by an AHRS. The angular velocity measurements were corrupted by zero-mean uncorrelated white Gaussian noise, with standard deviation of $0.05°/s$. The attitude is usually parametrized by roll, pitch, and yaw Euler angles, and as such noise in the attitude measurements was simulated by adding zero-mean, uncorrelated white Gaussian perturbations to the roll, pitch, and yaw, with standard deviation of $0.03°$ for the roll and pitch, and $0.3°$ for the yaw. It was assumed in the simulation that the relative position readings are provided by an Ultra-Short Baseline (USBL) positioning system, and as such each of those measurements is expressed in the body-fixed coordinates of the corresponding AUV, which means that each agent must apply its attitude matrix $\mathbf{R}_i(t)$ to the measurements to recover them in the inertial coordinate space.

The initial positions of the agents and the trajectory followed by the formation during the simulation are depicted in Fig. 7. As for the local observers, and also the centralized Kalman filter, the initial values for all state estimates were set to zero, except for the ones corresponding to the acceleration of gravity. As $\mathbf{g}_i$ is known approximately, it was set to its initial real value in all estimators to speed up the convergence of the estimation

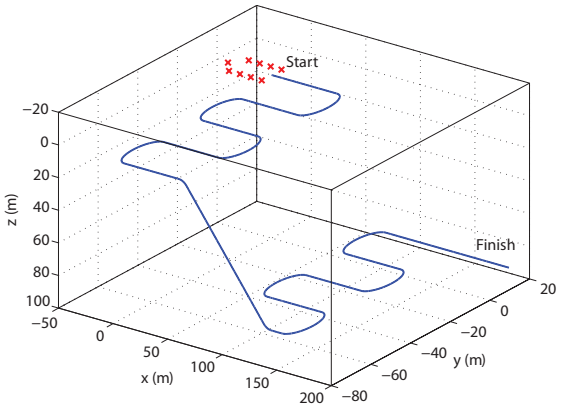

Figure 7: Initial positions of the agents and trajectory described during the simulation

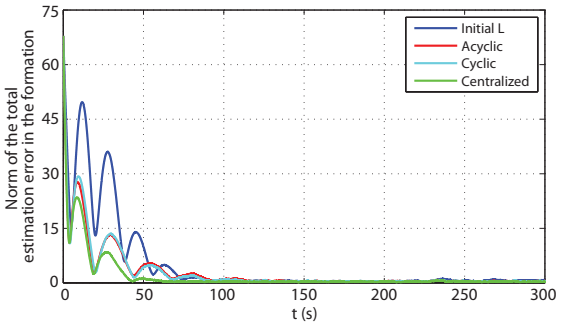

Figure 8: Evolution of the norm of the total estimation error in the formation

error. Nevertheless, these could have also been initialized at zero with no bearing on the stability and steady-state performance of the decentralized state estimator.

The results of the simulation are depicted in Figs. 8 through 11. Fig. 8 and Fig. 9 depict, respectively, the initial evolution and the steady-state behavior of the norm of the total estimation error of the formation. The results show that the performance of the non-improved state estimator is significantly worse than that of the other state estimators, and that the filter built on the cyclic formation graph achieves better results than the one built on the acyclic formation graph. This shows that the proposed algorithm is able to use additional measurements constructively, even if they render the formation graph cyclic.

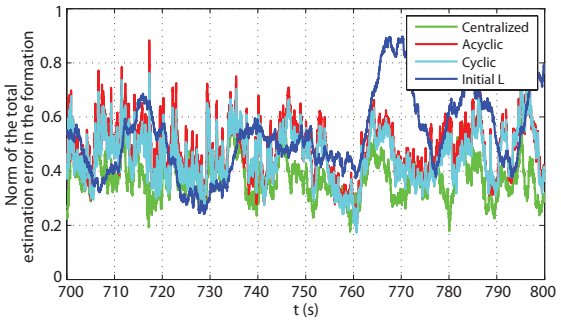

Figure 9: Detailed view of the norm of the total estimation error in the formation, once the initial transients have vanished

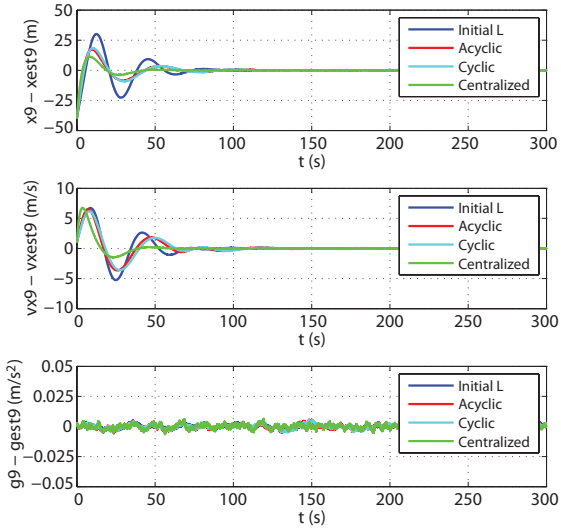

Figure 10: Evolution of the estimation error of agent 9

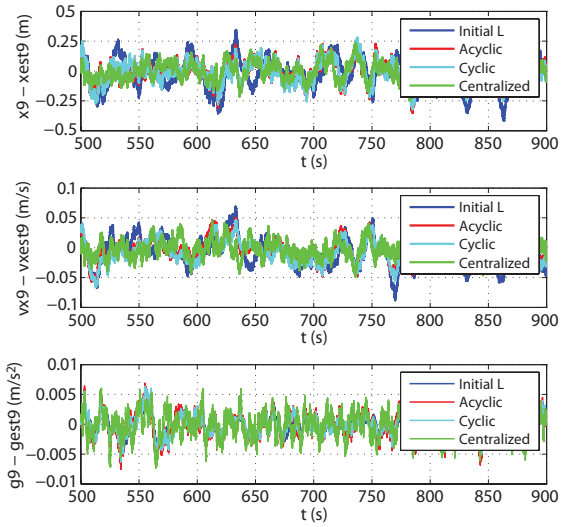

Figure 11: Steady-state estimation error of agent 9

Table 3: Standard deviation of the steady-state estimation error, averaged over 1000 runs of the simulation

	Initial $\mathbf{L}$	Acyclic	Cyclic	Centralized
$\sigma_{x_7}(\mathrm{m})$	1.66×10^{-1}	1.14×10^{-1}	1.08×10^{-1}	0.78×10^{-1}
$\sigma_{x_8}(\mathrm{m})$	1.63×10^{-1}	1.14×10^{-1}	1.08×10^{-1}	0.78×10^{-1}
$\sigma_{x_9}(\mathrm{m})$	1.47×10^{-1}	1.01×10^{-1}	1.04×10^{-1}	0.78×10^{-1}
$\sigma_{v_7}(\mathrm{m/s})$	3.04×10^{-2}	2.59×10^{-2}	2.21×10^{-2}	1.79×10^{-2}
$\sigma_{v_8}(\mathrm{m/s})$	3.03×10^{-2}	2.64×10^{-2}	2.25×10^{-2}	1.80×10^{-2}
$\sigma_{v_9}(\mathrm{m/s})$	2.82×10^{-2}	2.18×10^{-2}	2.29×10^{-2}	1.78×10^{-2}
$\sigma_{g_7}(\mathrm{m/s^2})$	1.68×10^{-3}	1.81×10^{-3}	1.50×10^{-3}	2.10×10^{-3}
$\sigma_{g_8}(\mathrm{m/s^2})$	1.66×10^{-3}	1.78×10^{-3}	1.49×10^{-3}	2.10×10^{-3}
$\sigma_{g_9}(\mathrm{m/s^2})$	1.58×10^{-3}	2.12×10^{-3}	1.87×10^{-3}	2.16×10^{-3}

Table 4: Measured total steady-state estimation error variance, averaged over 1000 runs of the simulation

	Initial $\mathbf{L}$	Acyclic	Cyclic	Centralized
$\sum\sigma^2$	0.3425	0.2542	0.2319	0.1481

Fig. 10 shows the initial evolution of the estimation error of agent 9, for the first coordinate of the position and velocity, and the third coordinate of the acceleration of gravity. As can be seen, in all cases the estimation error converges to the vicinity of zero after an initial transient caused by the mismatch of initial conditions. Fig. 11 depicts the steady-state behavior of the same estimation error variables, where the most discernible feature is the bad performance of the estimator with the non-improved $\mathbf{L}$ in comparison with the remaining filters.

To better assess the differences in performance between the four different state estimators, the Monte Carlo method was applied. The simulation was carried out 1000 times with different, randomly generated noise signals, and significant statistical data was extracted from the results and averaged over the 1000 simulations. The results are depicted in Table 3 and Table 4. Table 3 details the measured standard deviation of the steady-state estimation error for the first coordinate of the position and the velocity, as well as the third coordinate of the acceleration of gravity, for agents 7, 8, and 9, while Table 4 depicts the sum of the variance of all the steady-state estimation error variables in the formation. The data in both tables shows that the two improved decentralized state estimators perform clearly better than the filter with the non-optimized $\mathbf{L}$. There is also a smaller but still significant improvement in performance from the decentralized state estimator based on the acyclic graph to the one based on the cyclic graph, which once again suggests that the additional measurements, which render the formation graph cyclic, were incorporated constructively by the H_2 norm minimization algorithm. In this case, the two additional measurements led to a reduction of nearly 10% in the measured H_2 norm. The performance of the decentralized filters is worse than that of the optimal centralized filter, which is to be expected given the vastly inferior amount of information available to estimate the state of each individual agent. Nevertheless, the overall results are quite satisfactory for the decentralized estimation structure, which evidences the goodness of the proposed distributed solutions in comparison with the heavy computational and communication loads of the centralized estimator.

7. Conclusions

The problem of decentralized state estimation in formations of vehicles with fixed topologies was addressed in this paper. A method for designing computationally efficient local state observers presenting global error dynamics that converge globally asymptotically to zero was derived, and an algorithm for improving its H_2 nominal performance in the presence of noisy measurements or cycles in the graph associated with the formation was detailed. Finally, simulation results were presented that illustrate the performance of the proposed solution in noisy environments and the improvement resulting from the constructive use of additional measurements which render the formation graph cyclic.

Acknowledgments

This work was partially supported by Fundação para a Ciência e a Tecnologia (ISR/IST plurianual funding) through the PIDDAC Program funds, by the project PTDC/MAR/64546/2006 - OBSERVFLY of the FCT, and by the EU Project TRIDENT (Contract No. 248497).

References

[1] P. Barooah, Estimation and Control with Relative Measurements: Algorithms and Scaling Laws, Ph.D. thesis, University of California, Santa Barbara, 2007.

[2] J. N. Tsitsiklis, Problems in Decentralized Decision Making and Computation, Ph.D. thesis, Massachusetts Institute of Technology, 1984.

[3] Middleton, R.H. and Braslavsky, J.H., String Instability in Classes of Linear Time Invariant Formation Control With Limited Communication Range, IEEE Transactions on Automatic Control 55 (2010) 1519–1530.

[4] H. G. Tanner, G. J. Pappas, V. Kumar, Leader-to-Formation Stability, IEEE Transactions on Robotics and Automation 20 (2004) 443–455.

[5] J. A. Fax, Optimal and Cooperative Control of Vehicle Formations, Ph.D. thesis, California Institute of Technology, 2002.

[6] H. G. Tanner, D. K. Christodoulakis, Decentralized cooperative control of heterogeneous vehicle groups, Robotics and Autonomous Systems 55 (2007).

[7] R. Sousa, P. Oliveira, T. Gaspar, Joint Positioning and Navigation Aiding Systems for Multiple Underwater Robots, in: 8th IFAC Conference on Manoeuvring and Control of Marine Craft-MCMC 2009, Guaruja, Brazil, pp. 167–172.

[8] Y. Yuan, H. G. Tanner, Sensor Graphs for guaranteed cooperative localization performance, Control and Intelligent Systems (2010).

[9] F. Giulietti, L. Pollini, M. Innocenti, Autonomous formation flight, IEEE Control Systems Magazine 20 (2000) 34–44.

[10] J. D. Wolfe, D. F. Chichka, J. L. Speyer, Decentralized Controllers for Unmanned Aerial Vehicle Formation Flight, in: Proceedings of AIAA Conference on Guidance, Navigation, and Control.

[11] A. Healey, Application of formation control for multi-vehicle robotic minesweeping, in: Proceedings of the 40th IEEE Conference on Decision and Control, volume 2, pp. 1497–1502.

[12] T. B. Curtin, J. G. Bellingham, D. Webb, Autonomous Oceanographic Sampling Networks, Oceanography 6 (1993) 86–94.

[13] J. Bender, An overview of systems studies of automated highway systems, IEEE Transactions on Vehicular Technology 40 (1991) 82–99.

[14] D. Yanakiev, I. Kanellakopoulos, A Simplified Framework for String Instability Analysis in AHS, in: Proceedings of the 13th IFAC World Congress, volume Q, San Francisco, CA, USA, pp. 177–182.

[15] J. Kinsey, R. Eustice, L. Whitcomb, A Survey of Underwater Vehicle Navigation: Recent Advances and New Challenges, in: Proceedings of the 7th IFAC Conference on Manoeuvring and Control of Marine Craft, Lisboa, Portugal.

[16] P. Batista, C. Silvestre, P. Oliveira, Single Range Aided Navigation and Source Localization: observability and filter design, Systems & Control Letters 60 (2011) 665–673.

[17] P. Batista, C. Silvestre, P. Oliveira, A Sensor-based Long Baseline Position and Velocity Navigation Filter for Underwater Vehicles, in: Proceedings of the 8th IFAC Symposium on Nonlinear Control Systems - NOLCOS 2010, Bologna, Italy, pp. 302–307.

[18] C. Fransson, B. Lennartson, Low order multicriteria H_∞ design via bilinear matrix inequalities, in: Proceedings of the 42nd IEEE Conference on Decision and Control, volume 5, pp. 5161–5167.

[19] Y.-Y. Cao, Y.-X. Sun, W.-J. Mao, Output feedback decentralized stabilization: ILMI approach, Systems & Control Letters 35 (1998) 183 – 194.

[20] M. Morgado, P. Batista, P. Oliveira, C. Silvestre, Position USBL/DVL Sensor-Based Navigation Filter in the Presence of Unknown Ocean Currents, Automatica, in press (2011).

[21] P. Batista, C. Silvestre, P. Oliveira, Optimal position and velocity navigation filters for autonomous vehicles, Automatica 46 (2010) 767–774.

[22] P. Batista, C. Silvestre, P. Oliveira, Position and Velocity Optimal Sensor-based Navigation Filters for UAVs, in: Proceedings of the 2009 American Control Conference, Saint Louis, USA, pp. 5404–5409.
[23] R. W. Brockett, Finite Dimensional Linear Systems, Wiley and Sons, 1970.
[24] K. J. Astrom, R. M. Murray, Feedback Systems: An Introduction for Scientists and Engineers, Princeton University Press, 2008.
[25] W. D. Wallis, A Beginner's Guide to Graph Theory, Birkhauser, 2nd edition, 2007.
[26] D. B. West, Introduction to Graph Theory, Pearson, 2nd edition, 2001.
[27] B. Berger, P. W. Shor, Approximation algorithms for the maximum acyclic subgraph problem, in: Proceedings of the first annual ACM-SIAM symposium on Discrete algorithms, SODA '90, Society for Industrial and Applied Mathematics, Philadelphia, PA, USA, 1990, pp. 236–243.
[28] C. Scherer, S. Weiland, Linear Matrix Inequalities in Control, 2005.
[29] Toker, O. and Ozbay, H., On the NP-hardness of solving bilinear matrix inequalities and simultaneous stabilization with static output feedback, in: Proceedings of the American Control Conference, 1995, volume 4, pp. 2525–2526.
[30] D. B. Jazwinski, Stochastic Processes and Filtering Theory, Academic Press, 1970.